NASA Technical Memorandum 78814

DIRECTIVITY OF ACOUSTIC RADIATION FROM SOURCES

DONALD L. LANSING

JANUARY 1979

NASA
National Aeronautics and
Space Administration

Langley Research Center
Hampton, Virginia 23665

DIRECTIVITY OF ACOUSTIC RADIATION FROM SOURCES

Donald L. Lansing
Head, Aeroacoustics Branch
NASA Langley Research Center
Hampton, Virginia 23665

SUMMARY

This paper will describe the radiation properties of acoustic monopoles and dipoles. The directivity of radiation from these sources in a free field and in the presence of an absorptive surface is described. The kinematic effects on source radiation due to translation and rotation are discussed. Experimental measurements of sound from an acoustic monopole in motion and the characteristics of helicopter rotor and propeller noise are reviewed. The paper provides an introduction to several essential concepts required by noise control engineers making measurements of noise from moving sources in the proximity of the ground.

INTRODUCTION

When a noise source is brought near a surface or put into motion, a complex radiation pattern results which may be wholly unlike that of the source at rest in a free field. Acoustic measurements made of moving sources near surfaces for the purpose of characterizing the source behavior or understanding noise generating mechanisms must accordingly be corrected for motion and surface effects. A common example of this situation occurs when making measurements of noise from moving ground vehicles or aircraft during takeoff and landing. The effects of reflection and absorption of sound by the ground and the kinematic and dynamic effects of forward motion must be considered in the data analysis and subsequent interpretation.

This paper will survey the effects of the proximity of surfaces and the kinematic effects of motion, both translatory and rotational, on the directivity of radiation from acoustic monopoles and dipoles. The interference patterns and attenuation of sound from a source near an absorbing ground surface are explained. Three kinematic effects associated with uniform rectilinear motion, namely: retarded time, convective amplification, and Doppler shift, are described. An experimental study of the measurement of sound from an acoustic monopole in motion is discussed to illustrate the concurrence of surface and motion effects under controlled conditions. The paper surveys rotating blade noise radiation. The characteristic directivity patterns produced by blade thickness and aerodynamic forces, statically and in flight, are discussed to illustrate the features of propeller and rotor noise. General introductions to the kinematics of moving sources and helicopter noise are contained in references 1 and 2 respectively. The paper concludes with a brief review of several recent significant contributions to the theory of source radiation and its various applications. This paper provides useful background to the paper in this lecture series by Maestrello and Norum entitled, "Experimental Measurements of Moving Sources," and provides an introduction to several essential concepts required by engineers making and interpreting field measurements of noise from moving sources.

SOURCES OF SOUND

The sources of sound in a fluid can be introduced by considering the field equations of linearized acoustic theory. These equations, shown in Figure 1, are the continuity equation which expresses the conservation of mass, the momentum equation which describes the balance forces in the fluid, and the pressure-density relation which expresses the proportionality between the acoustic pressure and density perturbations. The term Q in the continuity equation accounts for the time rate of production of mass within the fluid. The vector whose components F_i appear in the momentum equation is any externally applied body force. These three equations can be combined into a single well known inhomogeneous wave equation.

In addition to the field quantities p, ρ, and u_i several quantities relating to energy and energy flux in the acoustic field need to be mentioned. These quantities are the acoustic intensity and acoustic power defined in Figure 2. The acoustic intensity is the time rate of sound energy flow across a unit area and is calculated by taking the time average of the product of the pressure and velocity component normal to the area. The acoustic power is the time rate of total energy flow through a closed surface completely surrounding the noise source and is a measure of the overall energy in the propagating sound field.

The nomenclature and definition of symbols given in Figures 1 and 2 will be used throughout the rest of this paper.

Figure 3 summarizes the principle sources of sound which occur within a completely linearized acoustic theory and present some practical examples of these sources. The differential operator on the left-hand side of the inhomogeneous wave equation describes the propagation of sound through a quiescent medium whose ambient speed of sound is c. The right-hand side of the equation consists of two terms which act as forcing functions to the wave equation and can be interpreted as producers of sound. These two terms represent the unsteady injection of mass into the medium and spatially varying applied body forces. Examples of the former type of sound source are unsteady or transient air jets and vibrating surfaces. Every element of a vibrating surface can be modelled as a piston which appears to insert and withdraw mass from the surrounding medium during its vibration. An important general class of examples of the second source is aerodynamic forces which develop upon bodies moving through a fluid. If nonlinear terms are included in the field equations, a third type of noise source arising from velocity fluctuations within the fluid itself can be derived. Examples of this noise source are turbulent fluid motions such as occur in jets, wakes and boundary layers. Thus, this type of source is central to flow noise generation. The production of noise by shear stresses will not be discussed in any great detail in this paper. The list of sound sources given here is not exhaustive. Other sources of sound in a fluid such as convecting density homogeneities, viscous shear stresses and enthalpy fluctuations are known. The reader is referred to the specialized literature for details.

The radiation from an acoustic monopole serves as a convenient reference to use in illustrating the effects of surfaces and motion on source directivity. The monopole represents the acoustic field produced by periodically injecting and withdrawing mass at a point in space with an angular frequency ω. The strength of the source, Q_0, is the time rate of mass injection. The acoustic pressure, radial velocity component, intensity and power are presented in figure 4 for convenience and will be referred to frequently throughout the paper to illustrate the changes surfaces and motion have upon the directivity of sources. A fact that will be used repeatedly is that the amplitude of the acoustic pressure for a monopole is constant on a sphere whose center is at the location of the monopole. Point harmonic generators of sound such as monopoles and dipoles (to be discussed subsequently) are central to the theory of acoustics since more complicated spatial and temporal distributions can be built up from these idealized sources by linear superposition. One expects then that the radiation properties of these point sources will then be carried over to more complicated distributions.

THE EFFECTS OF SURFACES ON SOURCE DIRECTIVITY

Consider first of all the influence of a nearby surface upon the directivity of sound from a monopole. A simple representation of this situation is shown in Figure 5 in which the surface is represented by a very large flat and perfectly reflecting plane. The boundary condition at the plane surface then is that the normal component of the acoustic velocity vanish at the surface. This situation in which a sound source is in the proximity of a large flat surface occurs for example during the landing approach or take-off operations of a commercial jet transport.

The mathematical solution of this radiation problem contains two terms, as shown in Figure 5. The first term represents the radiation field of the given monopole. The second term represents the radiation field of an image monopole placed directly below the actual source at an equal distance on the opposite side of the surface. At large distances from the source the equation for the radiation field can be considerably simplified as shown at the bottom of Figure 5. For the purposes of this discussion it is convenient to measure the distance R from the foot of the perpendicular from the source to the reflecting plane. If one compares the pressure fields obtained in this case with that of a free field monopole shown in Figure 4, it is seen that the amplitude of the pressure still falls off inversely with distance R but that the two equations differ by the directivity function $d(\theta)$ which is defined at the top of Figure 6. The pressure is no longer constant over a sphere of constant radius but is also a function of the observer's angular position θ, the source height h and the source frequency k. This nonuniform directivity comes about as a result of the superposition of the wave fields from the direct and image sources. The combined field has localized reinforcements and cancellations which produce a complex sound pattern.

The sketches at the bottom of Figure 6 illustrate the variation of the directivity function with observer angle and source frequency. The sketch on the left is a polar plot of the directivity function for a fixed source height and frequency. For a free space monopole the "directivity function" is a circle of unit radius. As the sketch shows the radiation field of a monopole near a surface produced by cancellations and reinforcements exhibits a lobed pattern for which pressure amplitudes can be locally twice as much as in the absence of the ground; moreover, there are angles at which the pressure amplitude drops completely to zero. The sketch at the right shows how the directivity function varies for fixed source and observer position as a function of frequency. It is seen that different frequencies undergo varying amounts of reinforcements and cancellation. Some frequencies experience complete reinforcement with pressure doubling; other frequencies show complete cancellation.

Ground surfaces such as grassland, or tilled soil are not perfectly rigid as is the idealized surface in the preceeding example. Most ground surfaces exhibit some degree of compliance to an incident acoustic wave. As suggested in Figure 7, an acoustic wave reflected from such a surface shows a decrease in amplitude due to sound absorption and a phase change produced by time lags in the sound-surface interaction process. These two physical phenomena are represented mathematically by a quantity known as the specific acoustic impedance which is characteristic of the particular type of surface. The specific acoustic impedance is a complex number which contains both amplitude and phase information. The real and imaginary parts of the impedance are known as the acoustic resistance and acoustic reactance, respectively. It is convenient to define a quantity called the specific acoustic admittance as the inverse of the specific acoustic impedance.

An alternate method of characterizing an acoustically absorbing surface is presented by L. Maestrello in the lecture entitled, "Experimental Measurements of Moving Sources." This method makes use of the notion of an acoustic transfer function between incident and reflected waves rather than that of an acoustic impedance. The two approaches are equivalent but the former technique appears to have the advantage in that the transfer function is more easily evaluated than the impedance over a broad frequency range.

Some measurements of the acoustic impedance of dry sand and grassland, taken from Reference 3, are shown in Figure 8. For these surfaces the acoustic resistance is nearly independent of frequency. The reactance on the other hand decreases significantly with increasing frequency over the range of measurements. The impedance of a surface may also vary with the angle of incidence of the sound wave. This effect is sometimes taken into account by defining an "effective" impedance as the product of the normal acoustic impedance and the cosine of the angle of incidence.

The far-field acoustic pressure for a source above an absorbing surface having a specific admittance ν is shown in Figure 9. The directivity function becomes considerably more complicated than for the perfectly reflecting surface. Directivity now depends on the surface properties as well as the source height and frequency and the observer location.

Some calculations of the directivity function $d'(\theta)$ for an absorbing surface are shown in Figure 10 and compared with the directivity for a perfectly reflecting surface. On the left is a polar plot of the directivity function for a fixed height and frequency and on the right is a plot as a function of frequency. The specific acoustic impedance used in the calculations, $4 - 4i$, is typical of the measurements shown in Figure 8. As can be seen from the two sketches, the effect of an absorbing surface on the directivity is

to reduce wave reinforcements so that pressure doubling does not occur. The frequencies at which pressure maxima and minima occur are increased significantly.

In summary then, there are several observations to be made regarding the effects of a surface upon the radiation from a source. The surface will produce a nonuniform directivity pattern due to the interference of sound waves from the source with waves reflected from the surface. These two wave fields interact with each other producing reinforcements at which the pressure is greater (up to two times) than the pressure in the free field and cancellations where the pressure can go nearly to zero. Compliant surfaces such as sand, soil, and grass tend to smooth out these reinforcements and cancellations somewhat and shift the frequency of their occurrence depending upon the impedance properties characteristic of that surface.

KINEMATIC EFFECTS OF MOTION ON SOURCE DIRECTIVITY

When a noise source is put into motion its radiation characteristics may be significantly different from those of the source at rest. There are two reasons for such differences: kinematic effects due solely to moving the source about in space and dynamic effects which may alter the noise generating process or radiation efficiency of the source. This section of the paper will consider the kinematic effect of uniform rectilinear motion on the directivity of source radiation. A second important class of moving sources, that is sources in rotation, will be considered subsequently in the paper. Moving sources occur frequently in noise measurement and noise control problems associated with transportation noise sources such as automobiles and aircraft.

Consider then the situation indicated in Figure 11. An aircraft is in constant velocity, constant altitude flight over an observer on the ground (for simplicity the surface effects discussed in the previous part of the paper will not be included in the discussion of this section). As the aircraft moves along the flight path beyond point A, the sound emitted at point A travels along the straight line joining point A to the observer. The aircraft arrives at point B when the sound emitted at point A arrives at the observer. That is, the observer simultaneously sees the aircraft at point B and hears the sound emitted at point A. Thus, for a moving source two source positions must be distinguished: the position at which the source is observed and the position of the source at which the detected sound was emitted. Let $\overline{R}$ be the distance between the observer and the emission point. The time taken for sound to travel this distance is $\frac{\overline{R}}{c}$. Consequently the sound heard at time t by the observer was actually emitted at an earlier time $t - \frac{\overline{R}}{c}$. This quantity $t - \frac{\overline{R}}{c}$ referred to as the retarded source time. The retarded time is the time at which the observed sound was emitted by the source. In order to deduce information about a moving noise source from far-field sound measurements one must associate the measured acoustic signatures at time t with the position and condition of the source at the corresponding retarded time.

Figure 12 gives the mathematical relationships between observation quantities and emission quantities and presents some sample calculations. The Mach number of the moving source is seen to be a fundamental parameter in the transformations. The sketch in the lower left shows the difference between the observation and emission angles as a function of the observation angle. The sketch at the right shows the ratio of the emission and observation distances. It can be seen that the difference between emission and observation quantities increases as the source Mach number increases. The difference between the source and observer angles is the greatest for overhead positions of the source. The ratio $\frac{\overline{R}}{R}$ is most sensitive to positions when the source is approaching and less sensitive when the source is departing in the distance.

Figure 13 shows the mathematical expression for the far-field acoustic pressure of a monopole in motion. This expression should be compared to that shown in Figure 4 for a stationary monopole. It is convenient in this situation to express the pressure in terms of the emission quantities $\overline{R}$ and $\overline{\theta}$. The pressure still falls off inversely with distance from the point of emission. However, the equation contains an additional directivity factor which is referred to as the "convective amplification factor." This factor is a function of the source Mach number and the emission angle $\overline{\theta}$. The equation implies that a monopole of fixed strength Q_0 will acquire directional radiation according to the convective amplification factor when it is set into uniform motion.

Figure 14 shows the effect of source Mach number upon the monopole directivity. It is convenient to consider the difference in sound pressure level between the moving monopole and the stationary monopole. The sketch gives a polar plot of this sound pressure level difference as a function of the emission angle for various Mach numbers. It can be seen that the sound pressure level increases significantly with Mach number in the direction of motion. There is a 16 dB increase for example directly ahead of the source at a Mach number of .6. There is also a decrease in the sound pressure levels behind the source. Note that convection effects are absent at 90° to the emission point. Far-field noise measurements for moving sources are frequently made at this 90° position in order to eliminate convection effects from the measured data.

The effects of source motion on the radiated acoustic power are shown in Figure 15. This figure shows a plot of the ratio of the power radiated at subsonic Mach number M to the value at zero forward speed (a quantity given in Figure 4) as a function of the source Mach number M. The simple algebraic expression for this ratio is given in the figure. The acoustic power associated with the moving monopole is calculated by determining the time average of the energy flux through a cylinder completely enclosing the path of motion as suggested by the sketch. It is seen from the plot that as the Mach number increases the radiated acoustic power also rapidly increases becoming infinite at sonic speed.

Another kinematic effect of motion on the radiation from a source is illustrated in Figure 16. This is the shift in the observed frequency of the radiation. The phase of the far-field acoustic pressure is determined by the expression $k\overline{R} - \omega t$. Introduce a cylindrical coordinate system (x, r) with the x axis coinciding with the line of source motion and the origin coinciding with the position of the source at time zero. In terms of these coordinates and the source velocity U and Mach number M the emission distance $\overline{R}$ can be written out explicitly as shown. The x, r coordinate system is a fixed set of coordinates in

space which then designate the observer position. In terms of these observer coordinates the phase of the acoustic pressure along the line of motion simplifies as indicated. Directly ahead of the source an observer will detect a frequency $\omega/(1 - M)$ where ω is the frequency of the moving source. This observed frequency is larger than the actual source frequency. Behind the source the observed frequency decreases by a factor of $1/(1 + M)$. For a general observation position the observed frequency is the time rate of change of the phase of the pressure. When the algebra is worked through the general expression for the observer frequency is that given at the bottom of figure 16. It is seen that in general the frequency is increased ahead of the emission point and is decreased aft of the emission point. Convective changes in frequency vanish at the 90° to the emission point.

In summary there are three kinematic effects of motion upon radiation from a source. There is the notion of retarded time, that is, that the observed sound was emitted at a time before it is measured at a point which is different from where the source is observed. The directivity of radiation from a source changes with the sound energy generally beamed in the direction of motion. And finally the observed frequency of a moving sound source may be larger than or less than the true source frequency depending upon the position of the observer with respect to the source.

It is important to reemphasize that these effects are solely due to the forward motion of the source and are independent of the nature and strength of the source. These effects must be corrected out of far-field acoustic data when the latter are used to diagnose the nature and condition of a complex unknown moving source. In particular convection effects must be distinguished from fundamental changes in the noise generation process which can come about due to forward motion. Far-field acoustic measurements are frequently used to diagnose the presence of such changes in the source. As seen from the equations in Figures 13 and 16, convection effects can be eliminated from the far-field directivity and Doppler shifts in frequency by making acoustic measurements at 90° to the emission point.

MEASUREMENTS OF SOUND FROM AN ACOUSTIC MONOPOLE IN MOTION

A moving source problem of considerable interest in connection with aircraft noise is the effect of forward motion upon the generation of jet noise. Changes in jet noise with forward motion occur due to both kinematic and dynamic effects. In an effort to understand kinematic effects as they occur in actual practice and to evaluate a theoretical model for predicting these effects an experimental study was carried out of the effects of forward speed upon radiation from a monopole, Reference 4. Both motion and surface effects which have been discussed individually in the previous sections of the paper make their appearance in this experimental study.

The monopole source was mounted on top of an automobile 7.9 meters above the ground atop a mast supported with guy wires as indicated in Figure 17. The source consisted of a 60 watt acoustic driver necked down through a 1.52 centimeter diameter tubular opening. The source radiated approximately uniformly in all directions when at rest. The output of this source consisted of tones of discrete frequency f. The automobile was driven at constant speeds U ranging from 13.4 to 44.4 meters per second.

Figure 18 shows a schematic of the experimental test setup. The automobile was driven along a straight track at constant velocity. The experiment was performed over an aircraft runway consisting of an asphalt surface. Sideline microphones were positioned at heights, h_0, of 3.05 meters and 6.10 meters above the ground surface. Pressure signals were measured with 1.3 centimeter diameter condenser microphones and recorded on magnetic tape.

A mathematical analysis of this problem was carried out for comparison with the experiment. The solution was obtained by the use of Fourier integral techniques and an application of the Lorentz transformation. The solution contains both surface reflection effects and convection effects. The next three figures show some results of the measurements and analysis made in this investigation.

Figure 19 shows a comparison between the calculated and measured noise time histories. The specific acoustic impedance of the runway surface used in the calculation is taken as $4 - 4i$. The sound pressure level in dB is plotted on the vertical scale. The horizontal scale is time normalized by means of the source velocity U and the source to observer distance at closest approach σ. The measured and computed curves are not superimposed here because of the many oscillations in the SPL's which are due to reinforcements and cancellations which come about due to ground reflection.

The smooth computed curve at the top of the figure is the predicted variation in the sound pressure level in the absence of a surface. As the source approaches the microphone the sound pressure level increases smoothly, reaches a maximum level at the point of closest approach, and then decreases gradually as the source moves away. In the presence of the ground surface both the computed and measured sound pressure levels show this general trend. However, superimposed upon this mean trend is a strong modulation due to the motion past the microphone of the complicated pattern of reinforcements and cancellations produced by ground reflection.

Figures 20 and 21 show the variation of the computed and measured noise time histories with observer height h_0 and source frequency. It can be seen that as either the observer height or the frequency of the source is increased the measured and computed SPL's become more and more oscillatory as the distance between successive reinforcements and cancellations grows smaller.

ROTATING BLADE NOISE

Noise from rotating blades is a pervasive problem associated with ground transportation. Blade induced noise may cause vibration to vehicle structures, malfunction of onboard instrumentation and equipment, annoyance in passengers, vibration in nearby ground structures, and interference with crew performance. Aircraft having rotating blade components include CTOL, VTOL, general aviation, and supersonic transport vehicles. Examples of rotating blade components which produce noise are shown in Figure 22. These components include ducted fans and compressors as well as free rotors such as helicopter rotors and general aviation propellers. This section of the paper will survey the fundamentals of noise production and radiation from rotating sources.

The noise sources for rotating blades are shown in Figure 23. These sources are the aerodynamic forces such as torque, thrust, and coning which develop on the rotating blades and the thickness distribution of the blades. Thus, in general, rotating blades produce both monopole and dipole type noise. Both steady and unsteady aerodynamic forces may be generated on the blades. The former may occur for example on a rotor in hover having a very smooth and uniform inflow. The latter are produced for example by skewed inflow, or blade-vortex interaction. The sound field from a system of rotating blades is periodic in time with a period $\frac{1}{B\Omega}$ and periodic around the axis of rotation with period $\frac{1}{B}$ where B is the number of blades and Ω is the shaft speed. Therefore, the far-field acoustic pressure can be represented as a Fourier series as indicated at the bottom of Figure 23 in which P_n are the Fourier harmonics. The remainder of the paper will discuss the effects of blade operating conditions on the radiation shapes associated with these individual sound harmonics.

Since some of the noise radiated from rotating blades is generated by blade aerodynamic loads, Figure 24 which summarizes the properties of radiation from a stationary dipole is included for reference. An acoustic dipole represents the acoustic effect due to the application at a point of a concentrated applied force which varies harmonically with time at angular frequency ω. In this figure the force is applied at the origin in the direction of the z axis. The resulting acoustic pressure is given by the z derivative of the pressure for a monopole. The directivity function in the far field is given by the cosine of the angle ψ between the axis of the force and the position vector to the observer. As indicated by the sketch at the bottom of Figure 24, the radiated noise is a maximum along the line of action of the force. The pressure vanishes everywhere in a plane normal to the force axis and passing through the point of application of the force.

The basic equation for the classical theory of propeller and rotor noise is shown in Figure 25. In this theory it is assumed that the inflow to the rotor is extremely clean and smooth so that the blade load distribution does not vary with time and that the rotor is stationary with respect to the surrounding air. An element of area of the rotor disc receives an impulse each time a blade passes. These impulses are represented by a distribution of monopoles and dipoles over the disc properly phased to take into account the time interval between successive blade passages. The amplitudes of the monopoles are determined by the blade thickness distribution whereas the amplitudes of the dipoles are obtained from the rotor thrust and torque distributions. The amplitude of the nth sound harmonic, $P_n(R, \psi)$ depends upon the rotor operating conditions and the observer position as shown in the equation.

The characteristic directivity patterns for these harmonics are shown in Figure 26. This figure contains schematic diagrams of the rotational noise radiation patterns for the thickness, thrust, and torque terms contained in the equation. These radiation patterns should be compared with those for a stationary monopole and dipole shown in Figures 4 and 24 respectively. For these sketches the rotor orientation illustrated at the top of the figure applies, that is, the axis of rotation is vertical and the plane of rotation is horizontal. The noise due to torque and thickness is a maximum in the plane of rotation and a minimum on the axis. The noise due to thrust has a four leaf clover pattern with pressure minima in the plane of rotation and on the axis.

The theory of propeller and rotor noise was modified by Garrick and Watkins to include the effects of propeller forward speed, Reference 5. The expression for the nth sound harmonic is given in Figure 27. The equation again assumes a clean inflow to the rotor which is in uniform forward motion at a Mach number M. The equation is expressed in terms of the emission distance $\overline{R}$ and angle $\overline{\psi}$ of the observer. A convective amplification factor is evident for each harmonic for thickness, thrust, and torque noise. Additional changes in the far-field directivity result from the presence of the forward Mach number in the argument of the Bessel function.

Figure 28 shows the changes which result in rotor noise radiation patterns due to forward motion. Sketches are given of the torque and thickness component and the thrust component of noise for three different low subsonic Mach numbers. The rotor orientation is as indicated at the top of the figure. The rotor is moving from left to right. The plane of rotation is vertical. For simplicity only half of the radiation pattern is shown. The complete pattern is of cource symmetric about the axis of rotation. Even at relatively modest forward speeds very significant beaming of the sound in the direction of motion occurs. Noise produced by torque and thickness is also increased in and behind the plane of rotation. There is little change in noise produced by thrust in the aft quadrant.

RECENT DEVELOPMENTS IN SOURCE RADIATION THEORY

The ideas described in the previous part of this paper have been well known and accepted for many years. Several more recent developments in the fundamental theory and application of source radiation deserve mention. The work of References 6 through 12 is recommended to the reader who wishes to familiarize himself with some of the current directions, controversies, and problems relating to source radiation.

Lowson, Reference 6, has developed an analysis for the radiation from monopoles, dipoles, and quadrupoles in arbitrary motion. His theory has been applied to explaining noise radiation from rotors due to unsteady blade loads, Reference 7. Unsteady blade loads result from rotor-stator interaction in turbofan aircraft engines or from blade-vortex interaction in free rotors. Unsteady blade loads have been found to be a very significant source of noise whenever they occur.

F. Farassat has derived expressions for the acoustic field of bodies of arbitrary shape and motion, Reference 8. Required parameters for noise prediction are the body geometry, time history of the motion, and surface pressure distribution. The compactness of the sources is not assumed. The analysis is carried out in the time domain and does not require decomposing the noise field into harmonics. The theory is particularly suitable for the prediction of impulsive noise from bodies such as high speed blade slap from helicopter rotors, Reference 9. Such noise is particularly difficult to handle and understand using Fourier analysis because of the presence of many high harmonics.

Lansing and Drishler, References 10 and 11, have obtained expressions for the sound field of a ducted propeller or rotor. The acoustic field within the duct due to rotating blades is expressed as a superposition of modes appropriate to the duct geometry. Corrections to account for the radiation into the free field are derived. This work is useful in analyzing the problem of aircraft engine noise propagation and radiation from internal rotating machinery.

A. Dowling, Reference 12, has recently published a new analysis of the radiation from a convecting monopole. The monopole is represented as a pulsating compact body which interacts with the surrounding fluid to produce both a mass and a momentum flux. The sound field from such a body has both a monopole and dipole component. Stronger convective amplification effects are obtained than for the simple monopole. It is also found that amplification in the direction perpendicular to the emission point may occur. The results raise some perplexing questions regarding the proper modeling of noise sources of practical importance.

CONCLUDING REMARKS

This paper has discussed the influence of the ground surface and motion - both rectilinear and rotational - on the directivity of radiation from acoustic sources. It was shown that interference patterns are produced by reflection and absorption at a surface and that consequently the far-field directivity of an acoustic source near the ground can be substantially altered from its free field value. The kinematic effects of motion which have been described are the beaming of sound in the direction of source motion and the shifting of the observer source frequency in a manner which is directionally dependent. Experimental data were shown to illustrate these effects. These phenomena explain some of the problems encountered in measuring noise from moving sources and the characteristics of noise from rotating blades. Reflection phenomena and kinematic effects of motion must be removed from noise data for moving sources near the ground in order to determine the characteristics of an unknown noise source and to investigate the dynamic effects of motion upon noise generation.

REFERENCES

1. Morse, Philip M.; and Ingard, K. Uno: Theoretical Acoustics. McGraw-Hill Book Company, 1968.

2. Richards, E. J.; and Mead, D. J.: Noise and Acoustic Fatigue in Aeronautics. John Wiley & Sons, Ltd., 1968.

3. Dickinson, P. J.; and Doak, P. E.: Measurements of the Normal Acoustic Impedance of Ground Surfaces. J. Sound & Vibration, vol. 13, no. 3, Nov. 1970, pp. 309-322.

4. Norum, T. D.; and Liu, C. H.: Point Source Moving Above a Finite Impedance Reflecting Plane - Experiment and Theory. J. Acoust. Soc. Am., vol. 63, no. 4, April 1978, pp. 1069.

5. Garrick, I. E.; and Watkins, Charles E.: A Theoretical Study of the Effect of Forward Speed on the Free-Space Sound-Pressure Field Around Propellers. National Advisory Committee for Aeronautics Report 1198, 1954.

6. Lowson, M. V.: The Sound Field for Singularities in Motion. Proc. Roy. Soc. (London), ser. A, vol. 286, no. 1407, Aug. 1965, pp. 559-572.

7. Lowson, M. V.; and Ollerhead, J. B.: A Theoretical Study of Helicopter Rotor Noise. J. Sound & Vibration, vol. 9, no. 2, 1969, pp. 197-222.

8. Farassat, F.: Theory of Noise Generation from Moving Bodies with an Application to Helicopter Rotors. NASA TR R-451, December 1975.

9. Farassat, F.; and Brown, T. J.: A New Capability for Predicting Helicopter Rotor and Propeller Noise Including the Effect of Forward Motion. NASA TM X-74037, June 1977.

10. Lansing, Donald L.: Exact Solution for Radiation of Sound from a Semi-Infinite Circular Duct with Application to Fan and Compressor Noise. Analytical Methods in Aircraft Aerodynamics. Symposium held at Ames Research Center, NASA SP-228, Oct. 28-30, 1969, pp. 323-334.

11. Drischler, Joseph A.: Analytical Studies of Sound Pressures Inside the Duct of Ducted Propellers. NASA TN D-6345, September 1971.

12. Dowling, Ann: Convective Amplification of Real Simple Sources. J. Fluid Mech. vol. 74, part 3, 1976, pp. 529-546.

ACKNOWLEDGEMENT

The author would like to thank Ms. Jean Mason for her help in carrying out many of the calculations shown in the figures.

CONTINUITY: $$\frac{\partial \rho}{\partial t} + \rho_o \frac{\partial u_i}{\partial x_i} = Q$$

MOMENTUM: $$\rho_o \frac{\partial u_i}{\partial t} = F_i - \frac{\partial P}{\partial x_i}$$

PRESSURE-DENSITY RELATION: $$P = c^2 \rho$$

INHOMOGENEOUS WAVE EQUATION $$\frac{1}{c^2} \frac{\partial^2 P}{\partial t^2} - \frac{\partial^2 P}{\partial x_i \partial x_i} = \frac{\partial Q}{\partial t} - \frac{\partial F_i}{\partial x_i}$$

ρ	DENSITY PERTURBATION	ρ_o, c	AMBIENT DENSITY AND SPEED OF SOUND
P	PRESSURE PERTURBATION	Q	TIME RATE OF PRODUCTION OF MASS PER UNIT VOLUME
u_i	VELOCITY COMPONENTS	F_i	COMPONENTS OF BODY FORCE PER UNIT VOLUME

Figure 1.- The Field Equations of Linearized Acoustics.

ACOUSTIC INTENSITY

TIME RATE OF ENERGY FLOW PER UNIT AREA

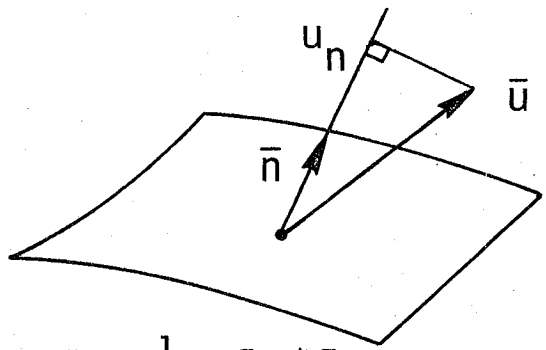

$$I_n = \text{TIME AVERAGE OF } \left[\mathrm{Re}(P)\mathrm{Re}(u_n)\right] = \frac{1}{2}\mathrm{Re}\left[P u_n^*\right]$$

ACOUSTIC POWER

TIME RATE OF TOTAL ENERGY FLOW THROUGH A CLOSED SURFACE

$$\text{II} = \iint_S I_n \, dS$$

Figure 2.- Energy Equations of Linearized Acoustics.

$$\underbrace{\frac{1}{c^2}\frac{\partial^2 P}{\partial t^2} - \frac{\partial^2 P}{\partial x_i \partial x_i}}_{\text{SOUND PROPAGATION}} = \underbrace{\frac{\partial Q}{\partial t} - \frac{\partial F_i}{\partial x_i}}_{\text{SOUND PRODUCTION}}$$

MATHEMATICAL EXPRESSION	PHYSICAL MEANING	EXAMPLES
$\frac{\partial Q}{\partial t}$	MASS INJECTION	UNSTEADY JETS VIBRATING SURFACES
$\frac{\partial F_i}{\partial x_i}$	BODY FORCES	AERODYNAMIC FORCES ON MOVING BODIES
IF NONLINEAR TERMS ARE INCLUDED IN THE EQUATION		
$\frac{\partial^2 (\rho u_i u_j)}{\partial x_i \partial x_j}$	SHEAR STRESSES	TURBULENT FLUID MOTIONS: JETS, WAKES, BOUNDARY LAYERS

Figure 3.- Sources of Sound.

$$Q = Q_0 \, \delta(x) \, \delta(y) \, \delta(z) \quad e^{-i\omega t}$$

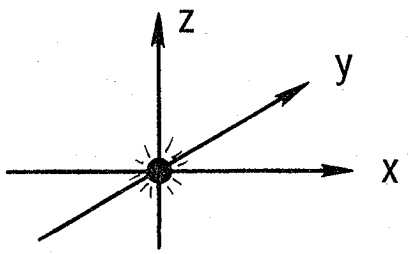

$$p = \frac{\omega Q_0}{4\pi i} \quad \frac{e^{i(kR - \omega t)}}{R} \qquad R^2 = x^2 + y^2 + z^2, \; k = \frac{\omega}{c}$$

$$u_R = \frac{1}{i\omega \rho_0} \frac{\partial P}{\partial R} = \frac{Q_0}{4\pi \rho_0} \quad e^{i(kR - \omega t)} \left[\frac{1}{R^2} - \frac{i k}{R} \right]$$

$$I_R = \frac{1}{2 \rho_0 c} \left(\frac{\omega Q_0}{4\pi R} \right)^2 = \frac{1}{2\rho_0 c} \quad |P|^2$$

$$II = \frac{\omega^2 Q_0^{\,2}}{8\pi \rho_0 c}$$

Figure 4.- Radiation from a Monopole.

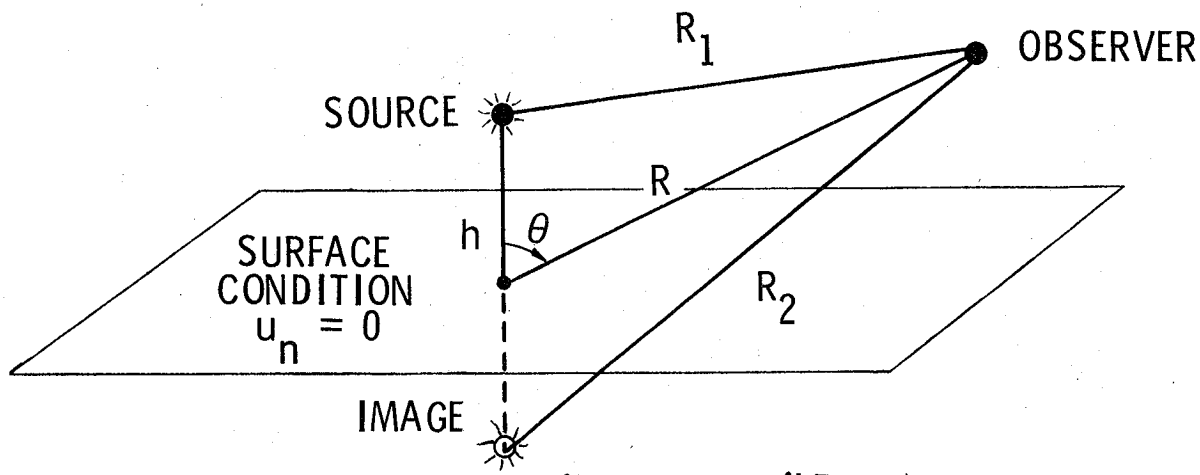

$$P = \frac{\omega Q_0}{4\pi i} \left\{ \underbrace{\frac{e^{ikR_1}}{R_i}}_{\text{ACTUAL SOURCE}} + \underbrace{\frac{e^{ikR_2}}{R_2}}_{\text{IMAGE SOURCE}} \right\} e^{-i\omega t}$$

IN THE FAR FIELD:

$$R_1 \approx R - h \cos\theta \ , \quad R_2 \approx R + h \cos\theta$$

$$P \approx \frac{\omega Q_0}{2\pi i} \cos(kh \cos\theta) \frac{e^{i(kR - \omega t)}}{R}$$

Figure 5.- Monopole Near a Reflecting Surface.

THE DIRECTIVITY FUNCTION

DIRECTIVITY FUNCTION: $d(\theta) = \left| 2 \cos (kh \cos \theta) \right|$

FIXED SOURCE HEIGHT AND FREQUENCY

f = 200 Hz h = 2.5 m kh = 9.1

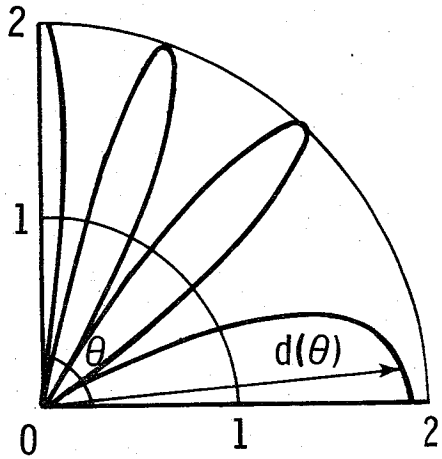

FIXED SOURCE AND OBSERVER POSITION

h = 2.5 m $\theta = 80^0$

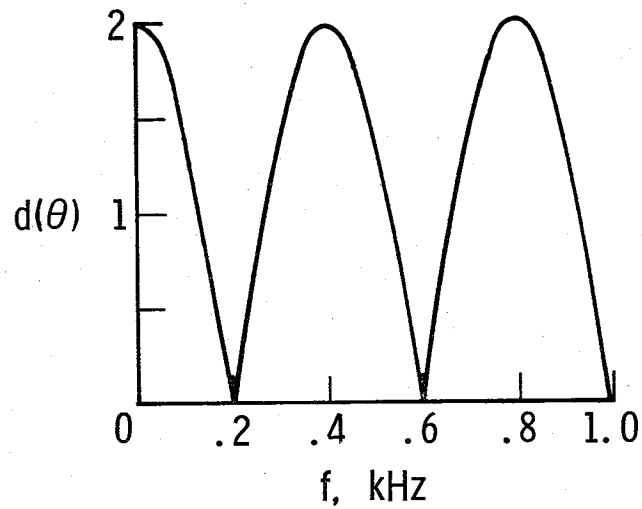

Figure 6.- The Directivity Function for a Monopole Near a Reflecting Surface.

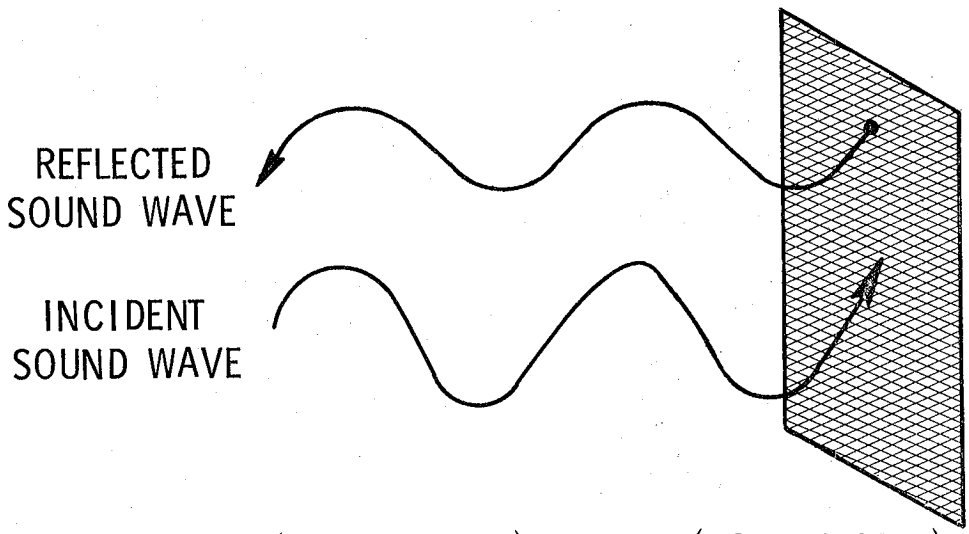

$$\text{SPECIFIC ACOUSTIC IMPEDANCE} = \left(\begin{array}{c}\text{SPECIFIC}\\ \text{RESISTANCE}\end{array}\right) - i \left(\begin{array}{c}\text{SPECIFIC}\\ \text{REACTANCE}\end{array}\right)$$

$$z = \frac{P}{\rho_0 c\, u_n} = \left(\frac{R}{\rho_0 c}\right) - i\left(\frac{X}{\rho_0 c}\right)$$

SPECIFIC ACOUSTIC ADMITTANCE: $\nu = 1/z$

Figure 7.- The Impedance of an Absorbing Surface.

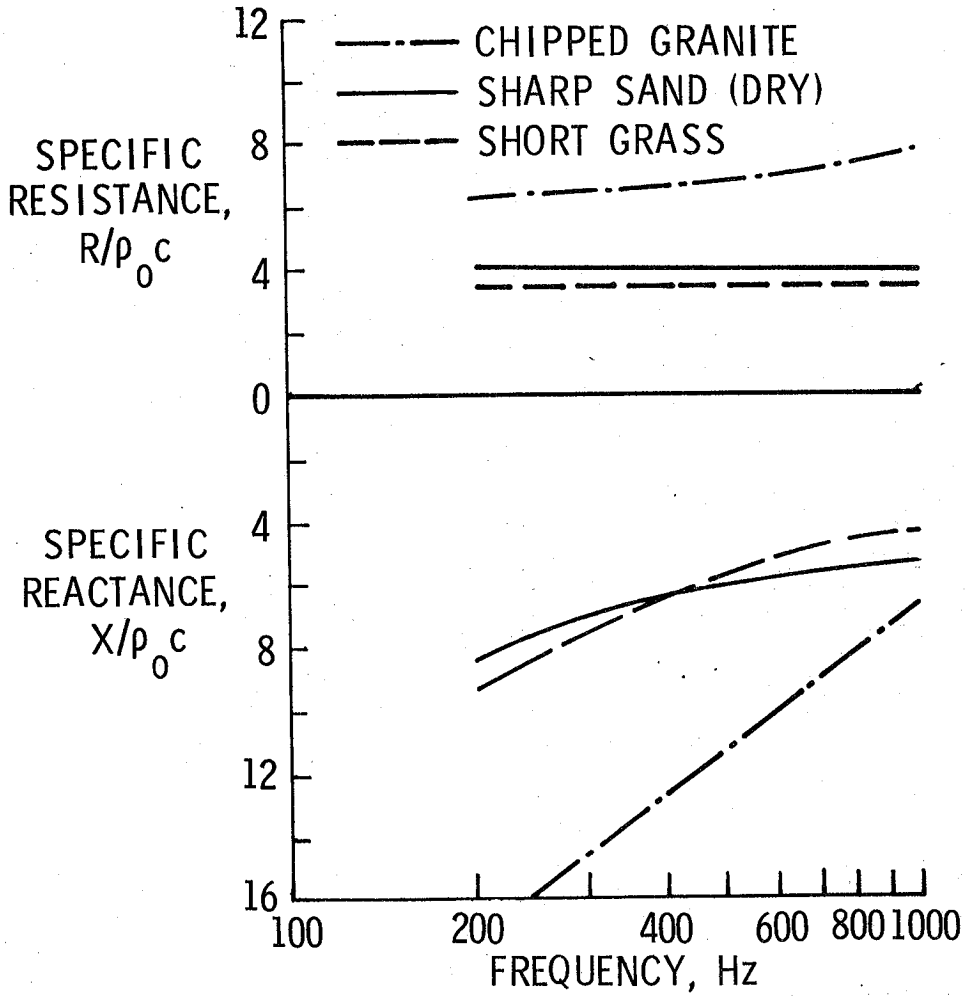

Figure 8.- Measured Acoustic Impedance of Ground Surfaces.

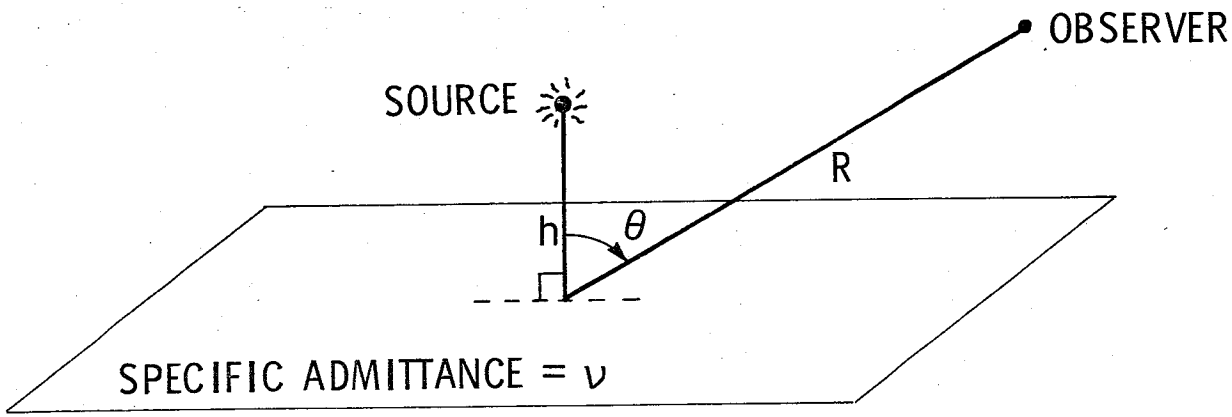

IN THE FAR FIELD:

$$P = \frac{\omega Q_0}{2\pi i} \left\{ \frac{\cos\theta \cos(kh\cos\theta) - i\nu \sin(kh\cos\theta)}{\cos\theta + \nu} \right\} \frac{e^{i(kR - \omega t)}}{R}$$

Figure 9.- Monopole Near an Absorbing Surface.

THE DIRECTIVITY FUNCTION

$$d'(\theta) = 2 \left| \frac{\cos\theta \cos(kh\cos\theta) - i\nu \sin(kh\cos\theta)}{\cos\theta + \nu} \right|$$

FIXED SOURCE HEIGHT AND FREQUENCY

f = 200 Hz h = 2.5 m kh = 9.1

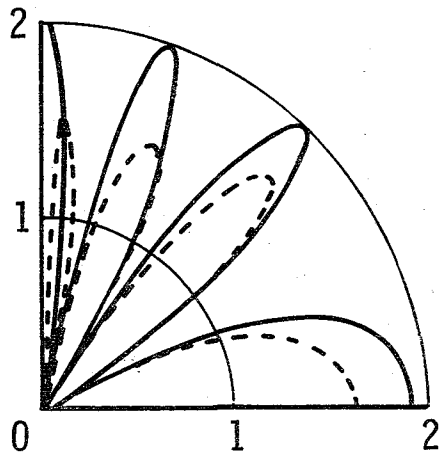

FIXED SOURCE AND OBSERVER POSITION

h = 2.5 m $\theta = 80^0$

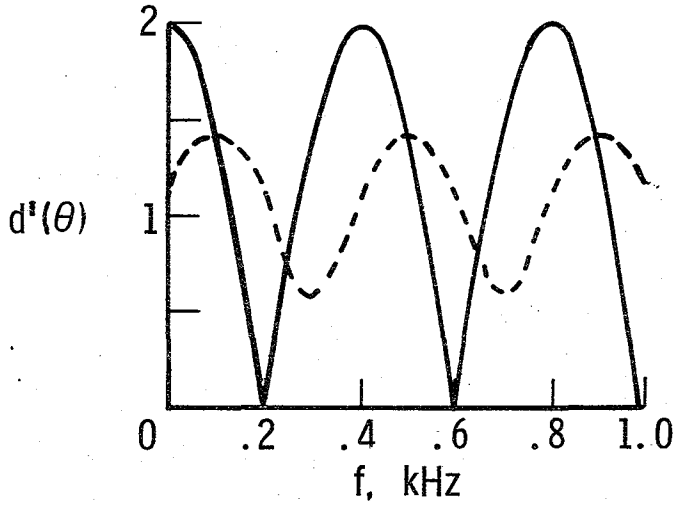

—— $\nu = 0$ (PERFECT REFLECTION) ----$\nu = 1/z = 1/(4 - 4i)$

Figure 10.- The Directivity Function for a Monopole Near an Absorbing Surface.

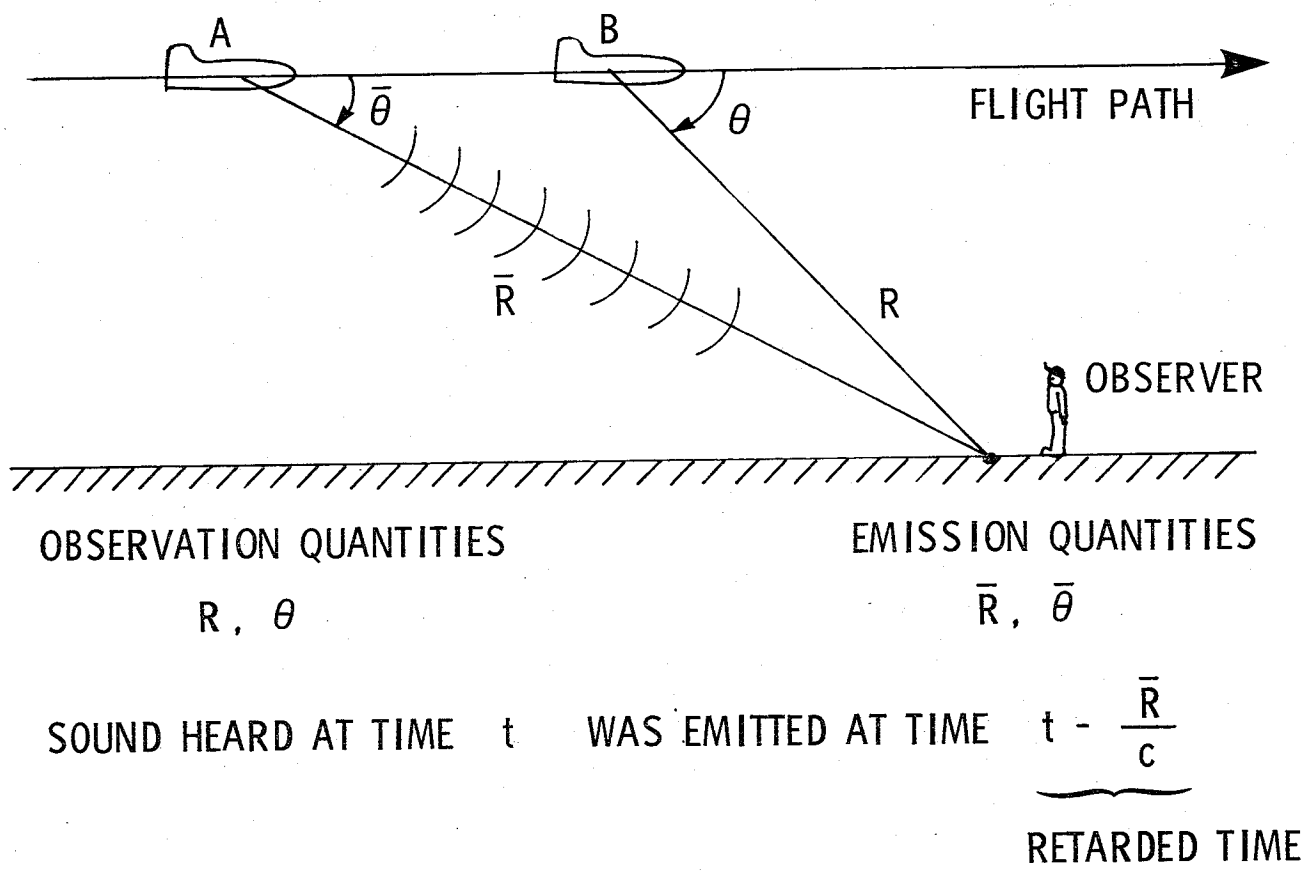

Figure 11.- The Effects of Motion on Source Radiation for Constant Altitude and Velocity Flight.

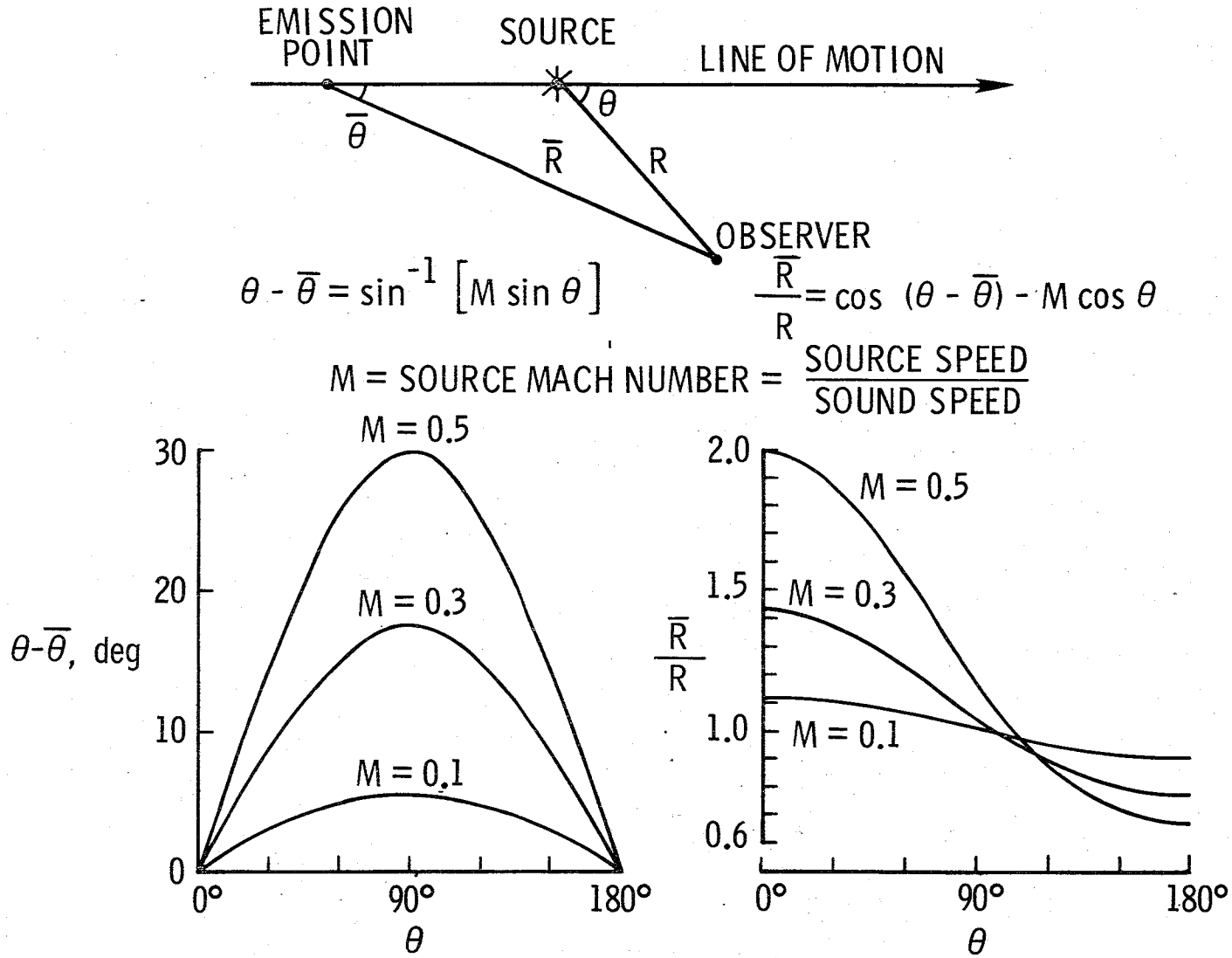

Figure 12.- Observer and Emission Quantities for Various Flight Mach Numbers.

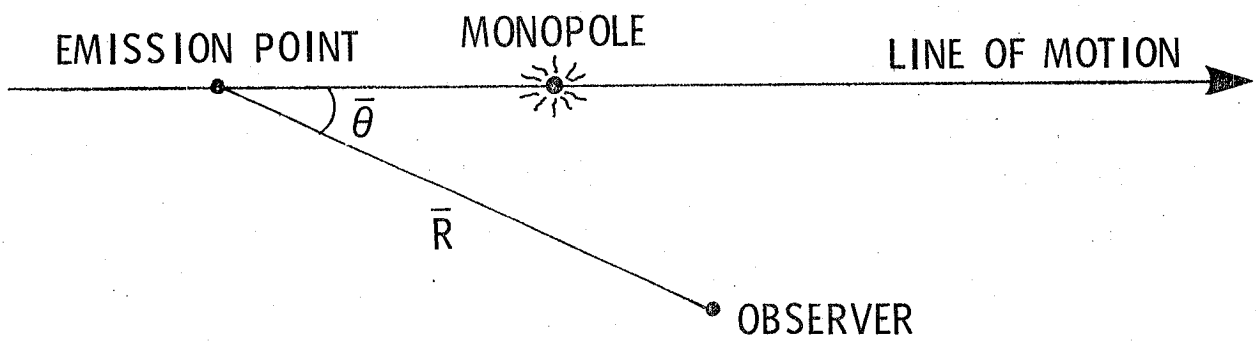

FARFIELD ACOUSTIC PRESSURE:

$$P \approx \frac{\omega Q_0}{4\pi i} \quad \underbrace{\frac{1}{(1 - M \cos \bar{\theta})^2}}_{\text{CONVECTIVE AMPLIFICATION FACTOR}} \quad \frac{e^{i(k\bar{R} - \omega t)}}{\bar{R}}$$

Figure 13.- Directivity of Radiation for a Monopole in Motion.

$$\Delta SPL = 20 \log \left[\frac{\text{MOVING SOURCE PRESSURE}}{\text{STATIONARY SOURCE PRESSURE}} \right] = -40 \log (1 - M \cos\bar{\theta})$$

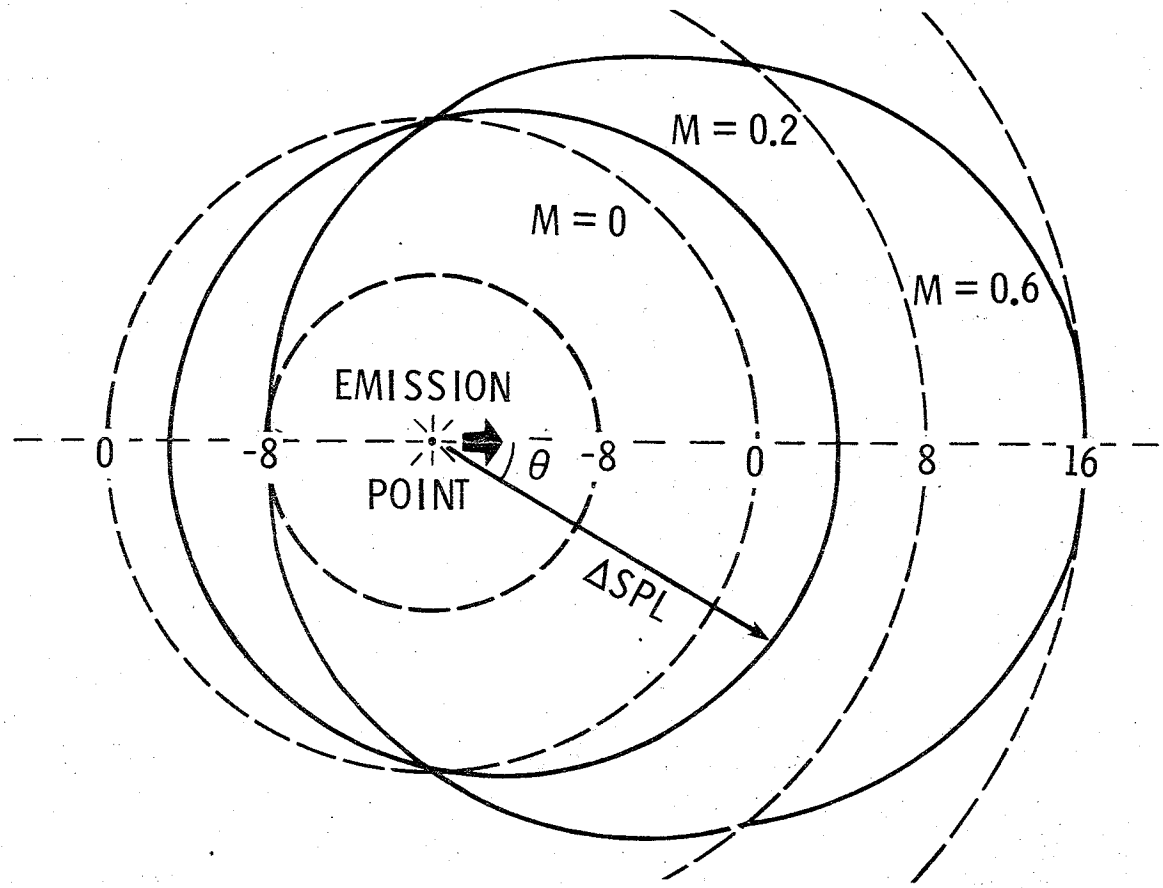

Figure 14.- Convection Amplification of Monopole Radiation.

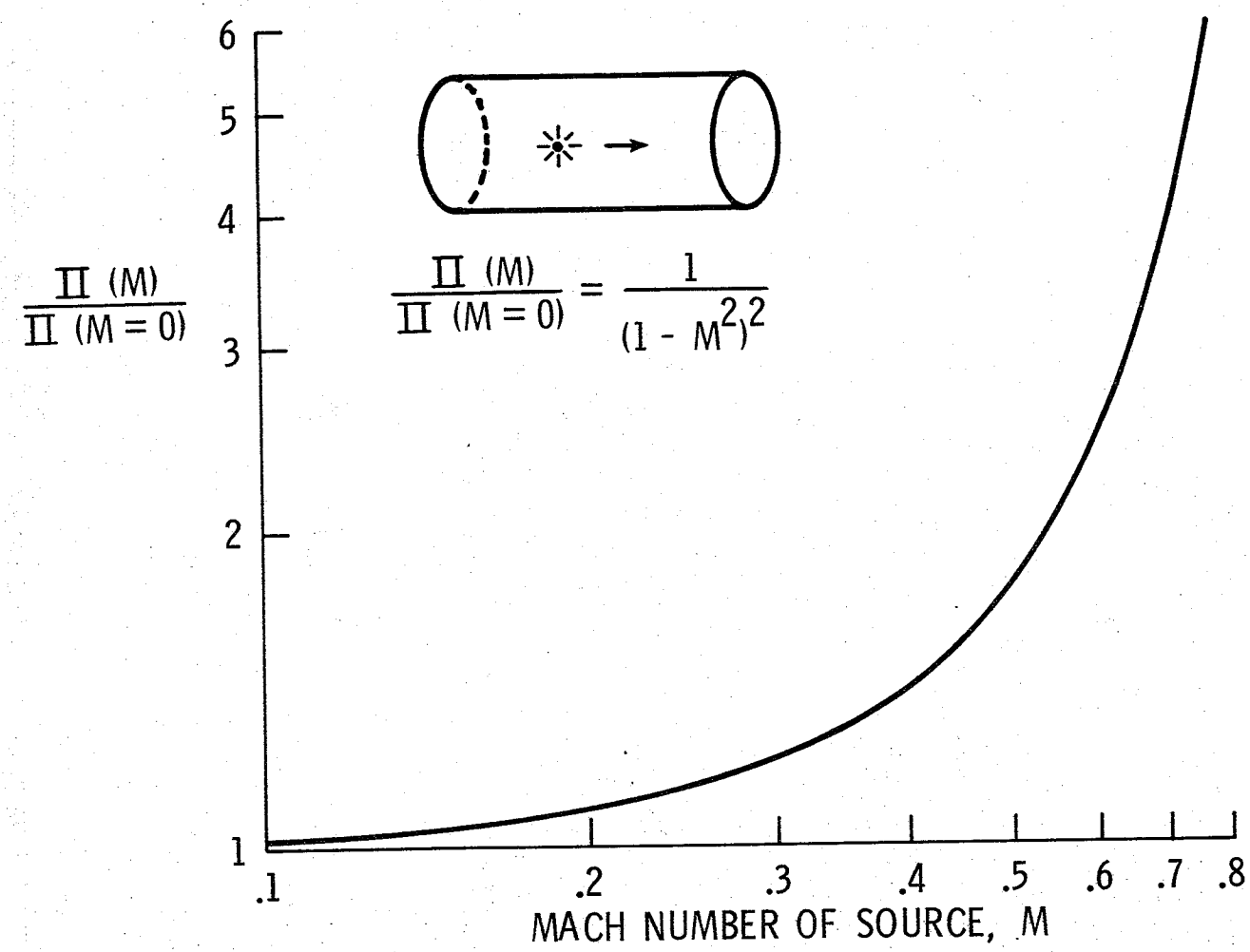

Figure 15.- Convective Amplification of Monopole Power

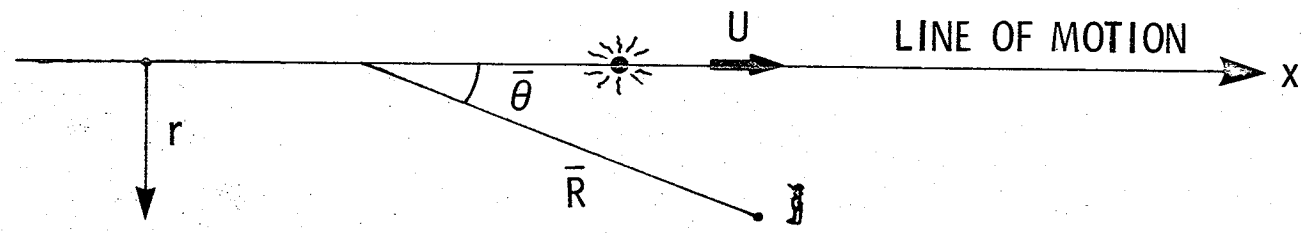

$$P \sim e^{i(k\bar{R} - \omega t)} \qquad \text{WHERE } \bar{R} = \frac{M(x - Ut) + \sqrt{(x - Ut)^2 + (1 - M^2)r^2}}{1 - M^2}$$

AHEAD OF THE SOURCE

$\bar{\theta} = 0,\ r = 0,\ x > Ut$

$$P \sim e^{i\left[\frac{k}{1-M}x - \frac{\omega}{1-M}t\right]}$$

OBSERVER FREQUENCY

BEHIND THE SOURCE

$\bar{\theta} = 180^0,\ r = 0,\ x < Ut$

$$P \sim e^{i\left[\frac{k}{1+M}x - \frac{\omega}{1+M}t\right]}$$

FOR A GENERAL LOCATION THE OBSERVER FREQUENCY, ω_o, IS :

$$\omega_o = \frac{d}{dt}(\omega t - k\bar{R}) = \frac{\omega}{1 - M\cos\bar{\theta}}$$

Figure 16.- Doppler Shift in Observation Frequency.

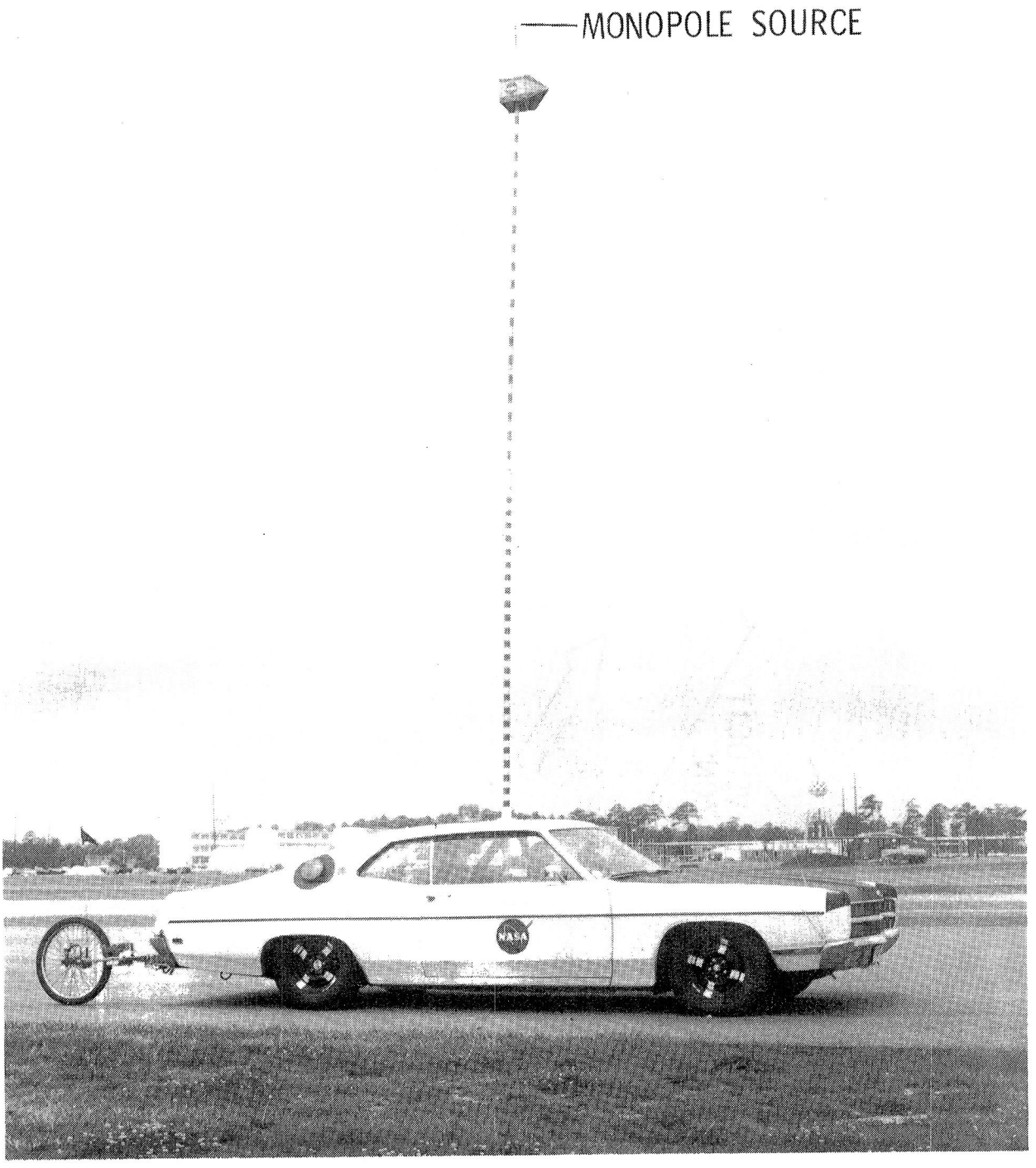

Figure 17.- Moving Monopole Source Experiment.

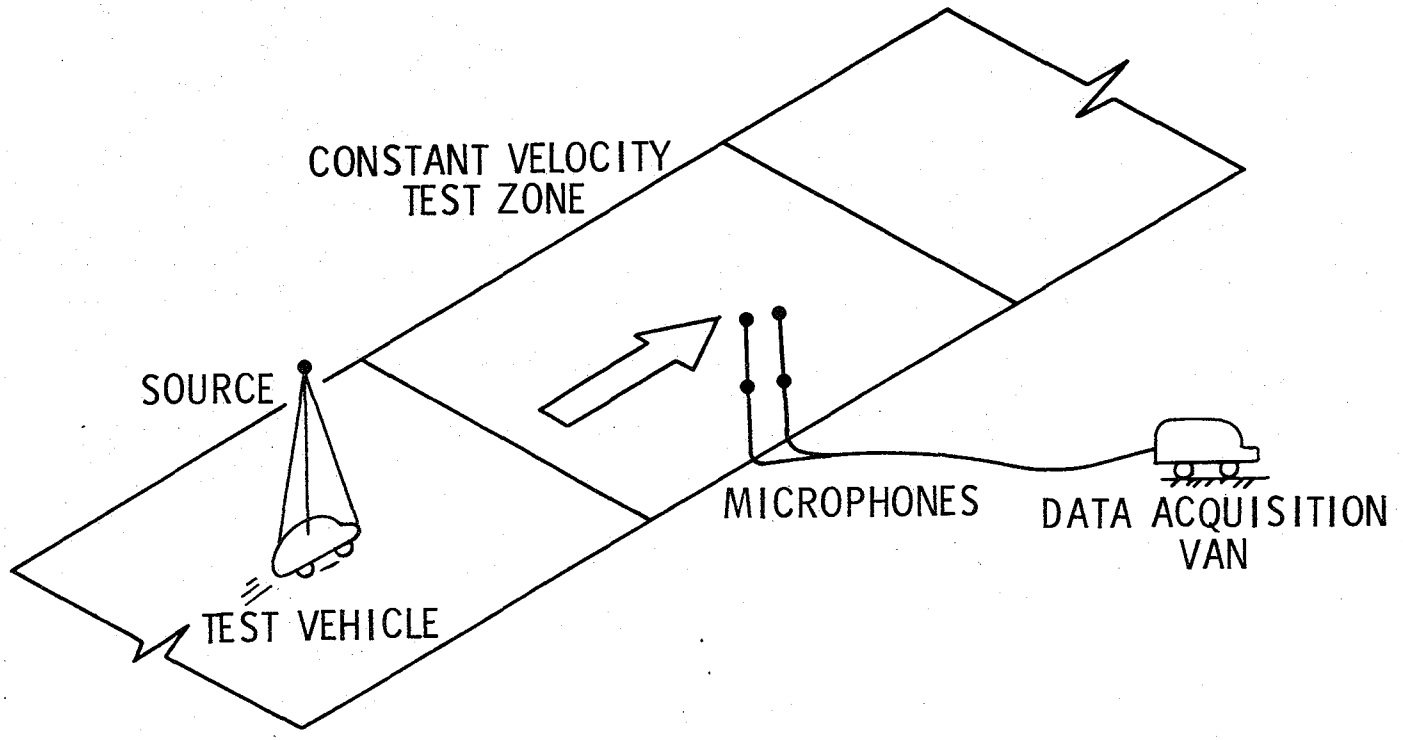

Figure 18.- Schematic of Test.

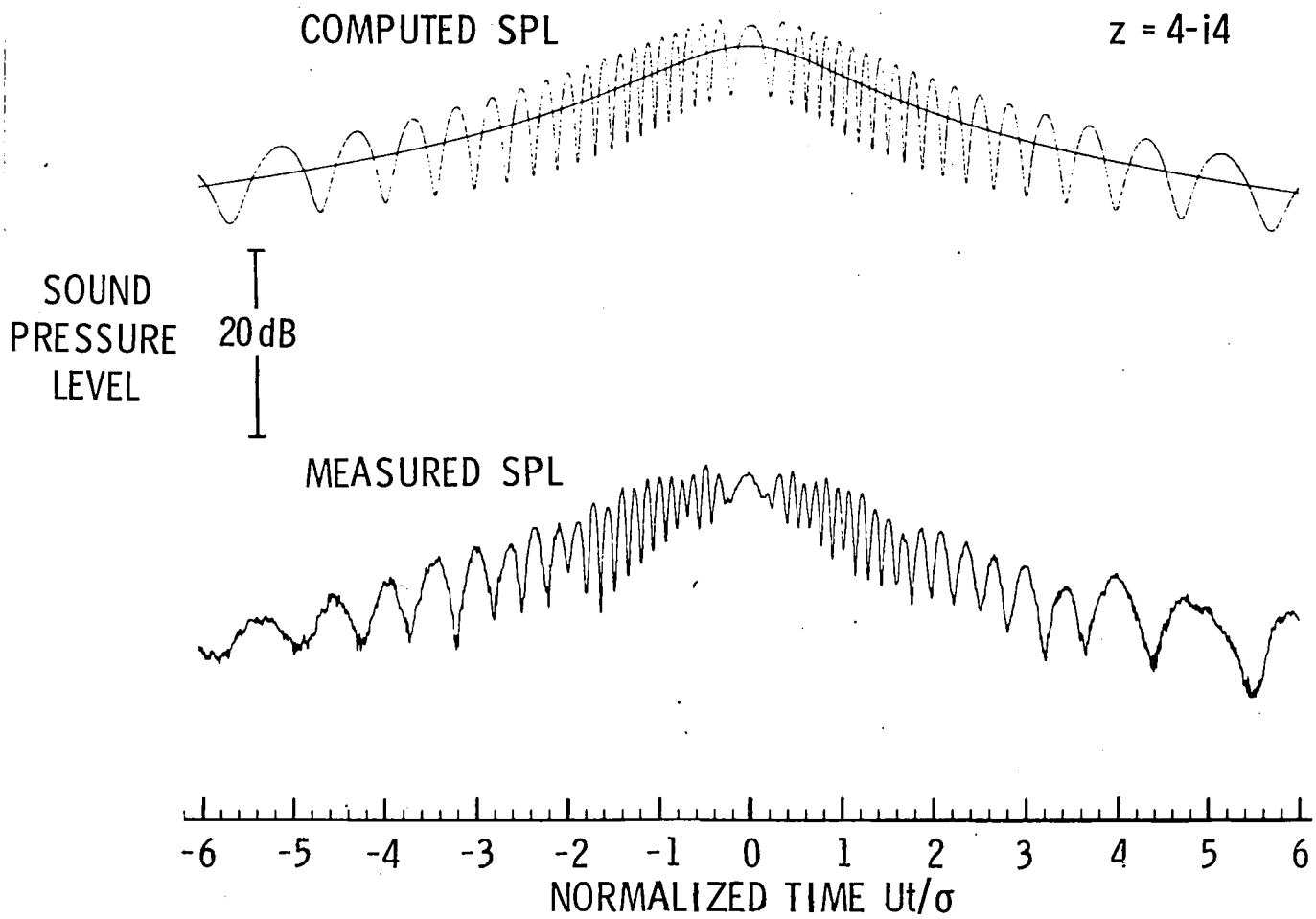

Figure 19.- Comparison of Theoretical and Experimental Noise Time Histories.
f = 1230 Hz, U = 13.4 m/s, h_0 = 6.10 m

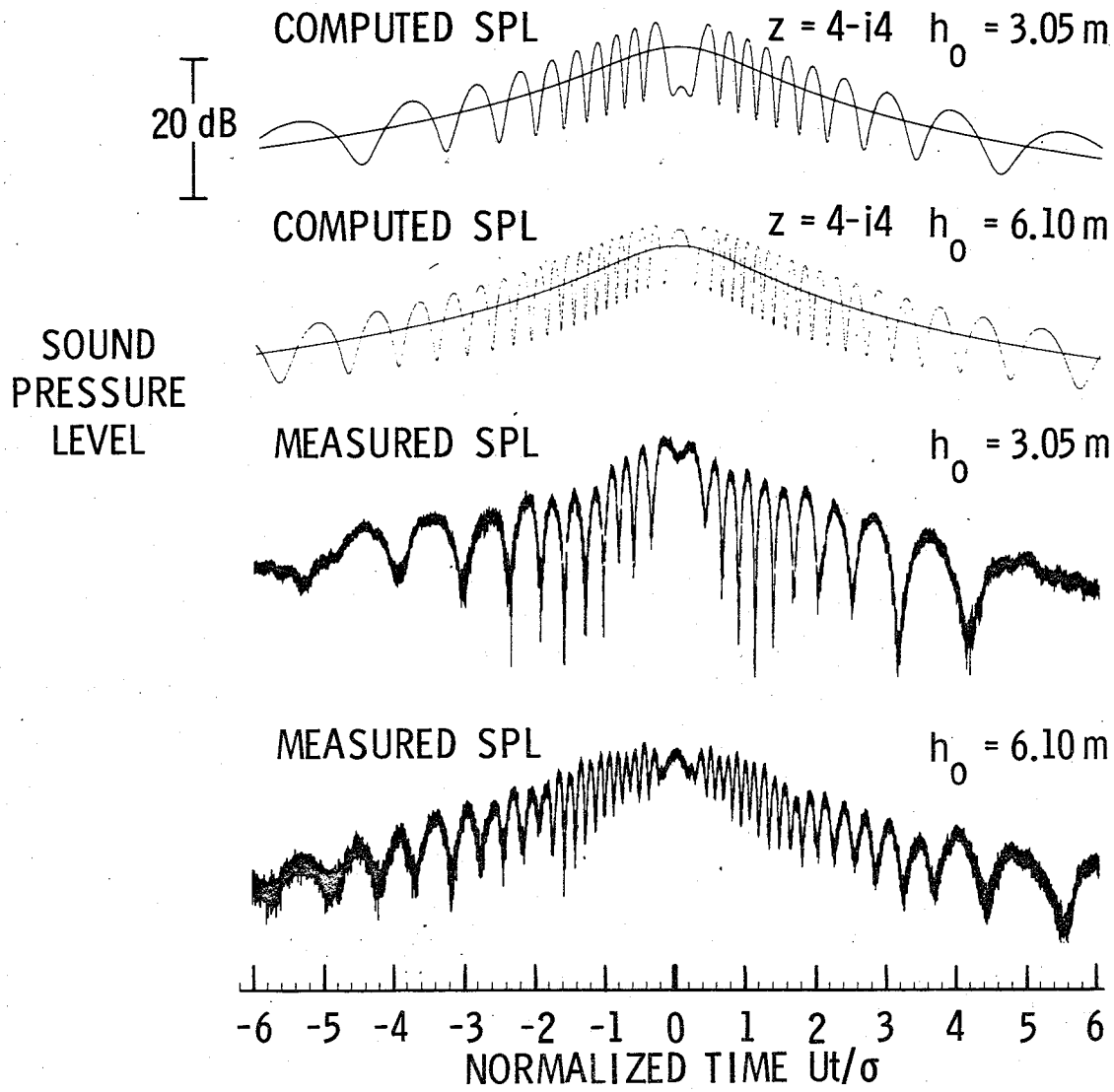

Figure 20.- Variation of Computed and Measured Noise Time Histories with Observer Height.
f = 1230 Hz, U = 13.4 m/s

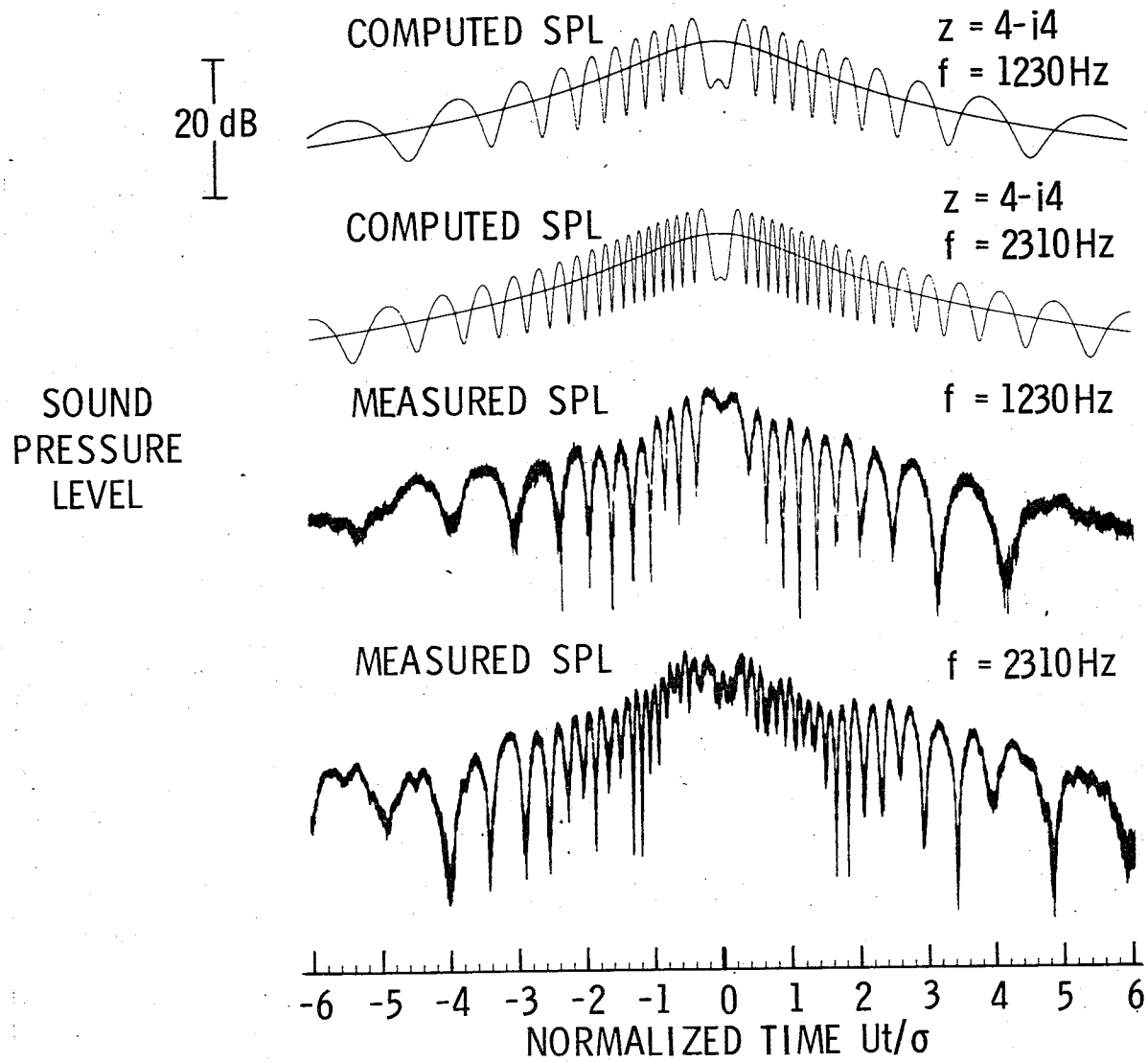

Figure 21.- Variation of Computed and Measured Noise Time Histories with Frequency.
U = 13.4 m/s, h_0 = 3.05 m

DUCTED ROTORS :

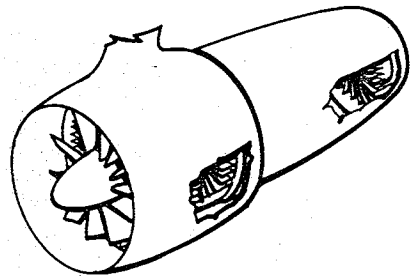

FAN - COMPRESSOR - TURBINE

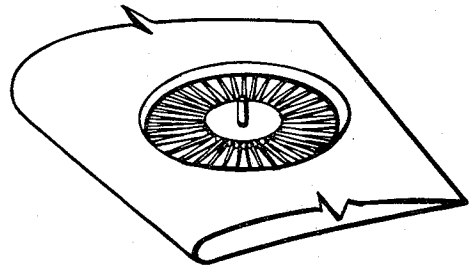

LIFT FAN

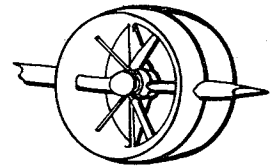

DUCTED PROPELLER

FREE ROTORS :

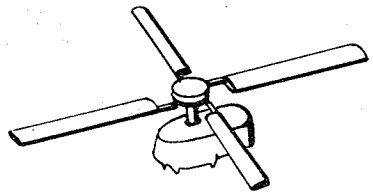

MAIN ROTOR

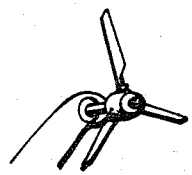

TAIL ROTOR

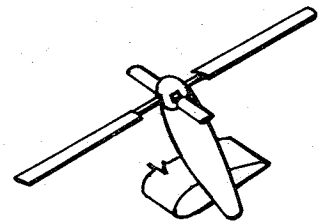

TILT ROTOR

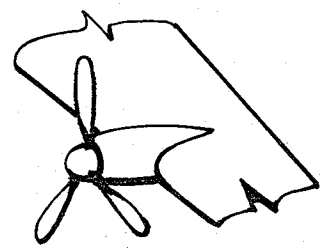

PROPELLER

Figure 22.- Rotating Blade Components.

TORQUE (Q)

THRUST (T)

CONING (C)

THICKNESS (q)

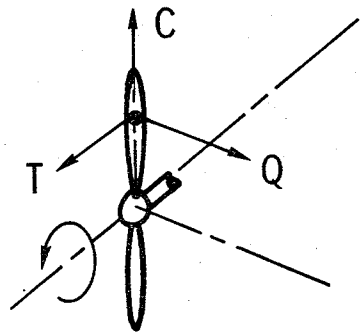

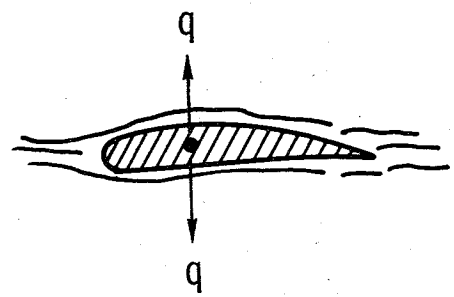

THE SOUND FIELD IS PERIODIC IN TIME AND SPACE AND CAN THEREFORE BE DEVELOPED IN A FOURIER SERIES:

$$P = \sum_{n=-\infty}^{+\infty} P_n e^{inB(\theta-\Omega t)}$$

Figure 23.- Noise Sources for Rotating Blades.

$$\bar{F} = F_z \, \delta(x) \, \delta(y) \, \delta(z) \, e^{-i\omega t} \, \bar{e}_z$$

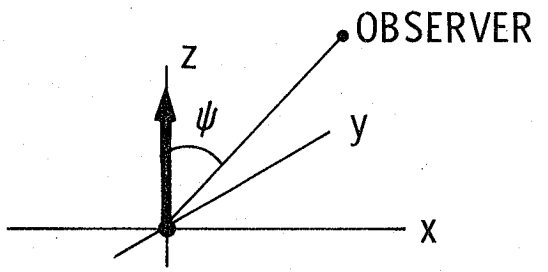

$$P = -\frac{3F_z}{4\pi} \frac{\partial}{\partial z} \left[\frac{e^{ikR}}{R}\right] e^{-i\omega t} \approx \underbrace{\frac{3kF_z}{4\pi i} \cos\psi \frac{e^{i(kR - \omega t)}}{R}}_{\text{IN THE FAR FIELD}}$$

DIRECTIVITY FUNCTION : $|\cos\psi|$

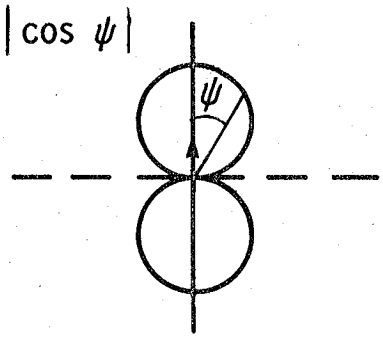

Figure 24.- Radiation from a Dipole.

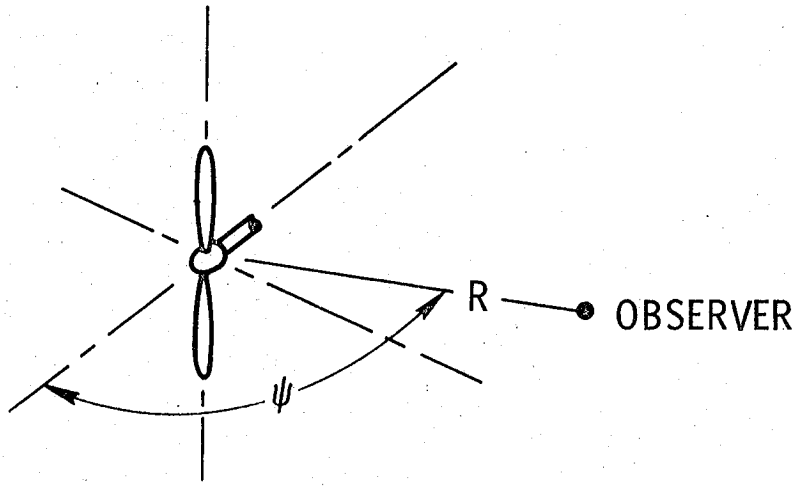

$$P_n(R,\psi) = \frac{nB\Omega}{2\pi cR}\left[cq + T\cos\psi - \frac{Q}{M_t R_e}\right] J_{nB}(nBM_t \sin\psi)$$

n	HARMONIC NUMBER	T	THRUST
B	BLADE NUMBER	Q	TORQUE
Ω	SHAFT SPEED	R_e	EFFECTIVE RADIUS
M_t	TIP MACH NUMBER	q	THICKNESS

Figure 25.- Noise Radiation Equations for Clean Inflow to a Hovering Rotor.

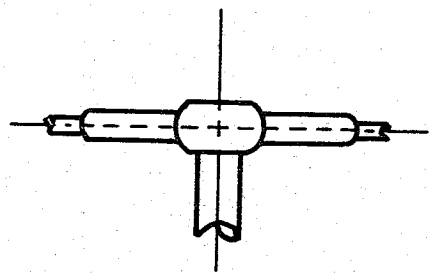

AXES THROUGH HELICOPTER HUB

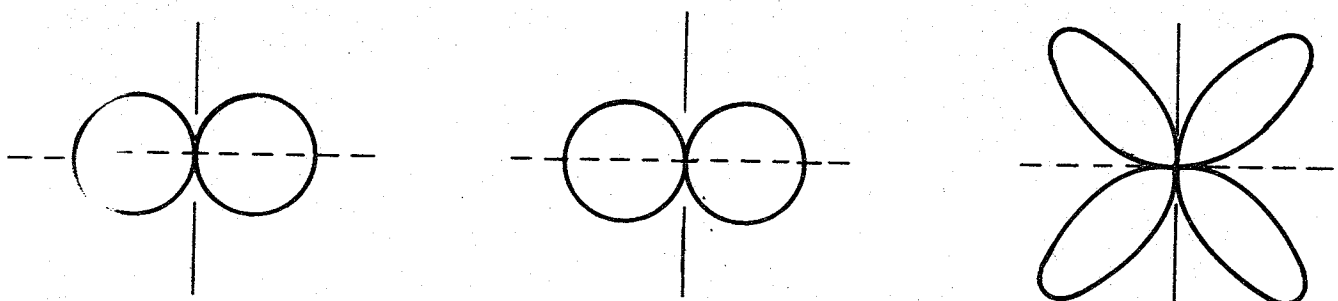

THICKNESS TORQUE THRUST

Figure 26.- Rotor Noise Radiation Patterns for Clean Inflow to a Hovering Rotor.

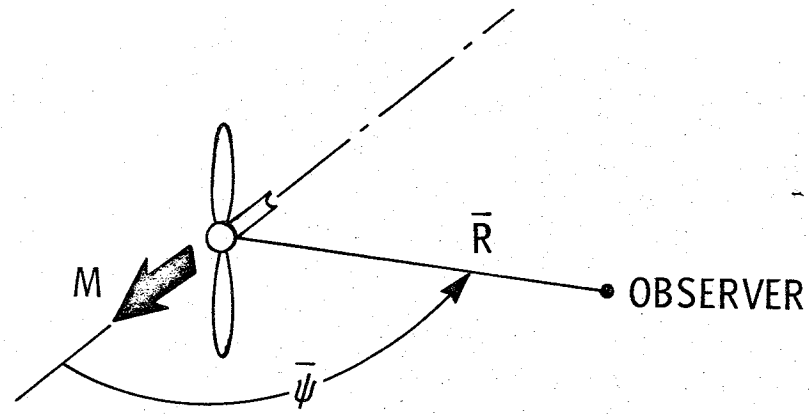

$$P_n(\bar{R}, \bar{\psi}) = \frac{nB\Omega}{2\pi c \bar{R}} \frac{1}{(1 - M^2)(1 - M\cos\bar{\psi})^2} \left[c\,q + T\cos\bar{\psi} - \frac{Q}{R_e M_t} \right] J_{nB}\left[nBMt \frac{\sin\bar{\psi}}{1 - M\cos\bar{\psi}} \right]$$

Figure 27.- Noise Radiation Equations for Clean Inflow to a Rotor in Forward Motion.

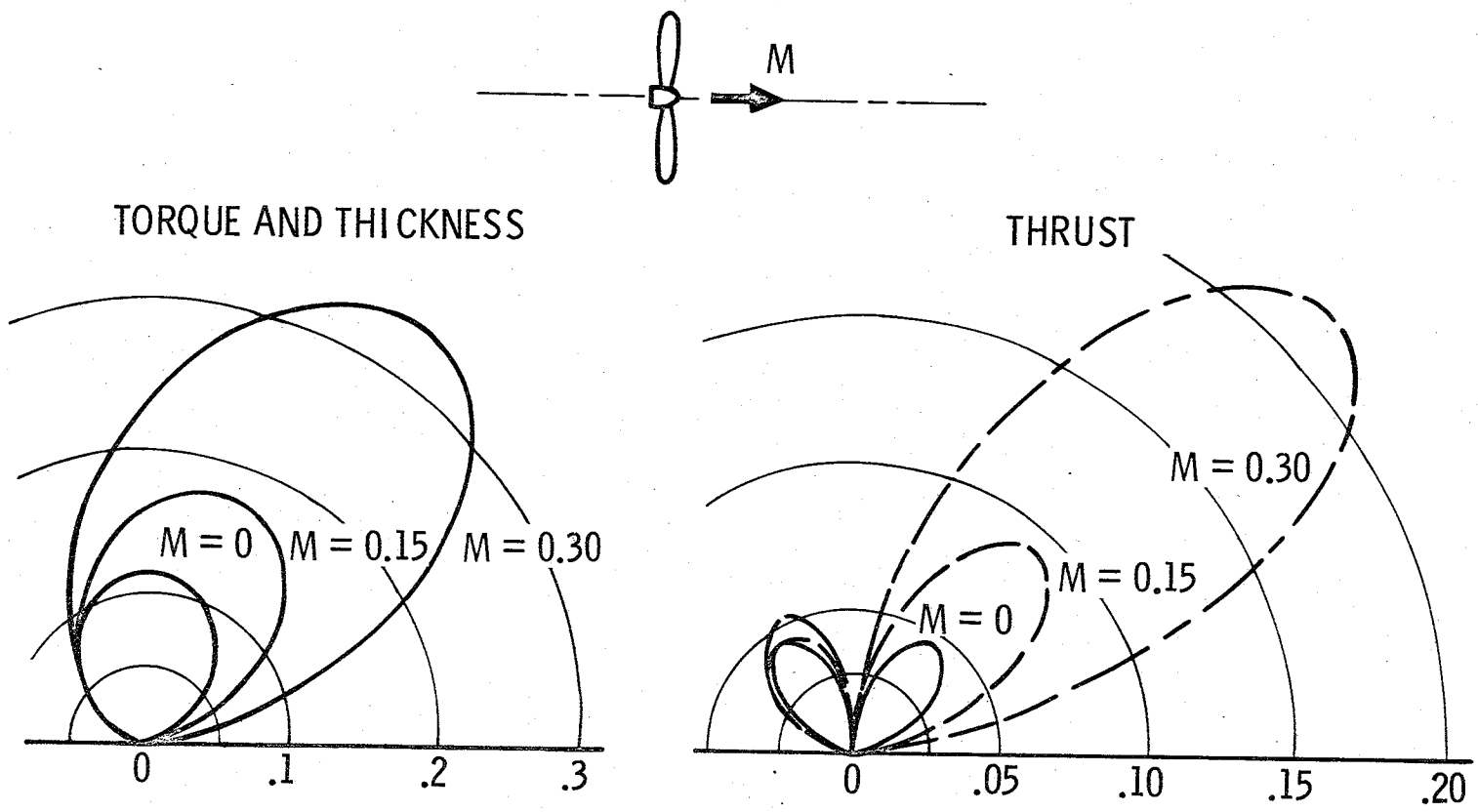

Figure 28.- Rotor Noise Radiation Patterns for Clean Inflow to a Rotor in Forward Motion

1. Report No.	2. Government Accession No.	3. Recipient's Catalog No.
NASA TM 78814		

4. Title and Subtitle	5. Report Date
Directivity of Acoustic Radiation From Sources	January 1979
	6. Performing Organization Code
7. Author(s)	8. Performing Organization Report No.
Donald L. Lansing	
9. Performing Organization Name and Address	10. Work Unit No.
NASA Langley Reseach Center Hampton, Virginia 23665	505-03-13-18
	11. Contract or Grant No.
	13. Type of Report and Period Covered
12. Sponsoring Agency Name and Address	Technical Memoradum
National Aeronautics and Space Administration Washington, DC 20546	14. Sponsoring Agency Code

15. Supplementary Notes

To be presented as a paper and included in the proceedings of the VKI/AGARD Special Course to be held in Brussels, Belgium, May 28-June 1, 1979

16. Abstract

This paper will describe the radiation properties of acoustic monopoles and dipoles. The directivity of radiation from these sources in a free field and in the presence of an absorptive surface are described. The kinematic effects on source radiation due to translation and rotation are discussed. Experimental measurements of sound from an acoustic monopole in motion and the characteristics of helicopter rotor and propeller noise are reviewed. The paper provides an introduction to several essential concepts required by noise control engineers making measurements of noise from moving sources in the proximity of the ground.

17. Key Words (Suggested by Author(s))	18. Distribution Statement
Noise Radiation Directivity of Acoustic Sources	Unclassified - Unlimited Subject Category 71

19. Security Classif. (of this report)	20. Security Classif. (of this page)	21. No. of Pages	22. Price*
Unclassified	Unclassified	34	$4.50

* For sale by the National Technical Information Service, Springfield, Virginia 22161